



Development and Validation of Arc Nanobodies: New Tools for Probing Arc Dynamics and Function

Yuta Ishizuka^{1,5} · Tadiwos F. Mergiya^{1,2} · Rodolfo Baldinotti^{1,2} · Ju Xu¹ · Erik I. Hallin¹ · Sigurbjörn Markússon¹ · Petri Kursula^{1,3,4} · Clive R. Bramham^{1,2}

Received: 21 January 2022 / Revised: 4 March 2022 / Accepted: 7 March 2022 / Published online: 20 March 2022
© The Author(s) 2022

Abstract

Activity-regulated cytoskeleton-associated (Arc) protein plays key roles in long-term synaptic plasticity, memory, and cognitive flexibility. However, an integral understanding of Arc mechanisms is lacking. Arc is proposed to function as an interaction hub in neuronal dendrites and the nucleus, yet Arc can also form retrovirus-like capsids with proposed roles in intercellular communication. Here, we sought to develop anti-Arc nanobodies (ArcNbs) as new tools for probing Arc dynamics and function. Six ArcNbs representing different clonal lines were selected from immunized alpaca. Immunoblotting with recombinant ArcNbs fused to a small ALFA-epitope tag demonstrated binding to recombinant Arc as well as endogenous Arc from rat cortical tissue. ALFA-tagged ArcNb also provided efficient immunoprecipitation of stimulus-induced Arc after carbachol-treatment of SH-SY5Y neuroblastoma cells and induction of long-term potentiation in the rat dentate gyrus in vivo. Epitope mapping showed that all Nbs recognize the Arc C-terminal region containing the retroviral Gag capsid homology domain, comprised of tandem N- and C-lobes. ArcNbs E5 and H11 selectively bound the N-lobe, which harbors a peptide ligand binding pocket specific to mammals. Four additional ArcNbs bound the region containing the C-lobe and C-terminal tail. For use as genetically encoded fluorescent intrabodies, we show that ArcNbs fused to mScarlet-I are uniformly expressed, without aggregation, in the cytoplasm and nucleus of HEK293FT cells. Finally, mScarlet-I-ArcNb H11 expressed as intrabody selectively bound the N-lobe and enabled co-immunoprecipitation of full-length intracellular Arc. ArcNbs are versatile tools for live-cell labeling and purification of Arc, and interrogation of Arc capsid domain specific functions.

Keywords Arc · N-lobe · C-lobe · Nanobody · Intrabody · Chromobody · Co-immunoprecipitation

Introduction

The immediate early gene encoding activity-regulated cytoskeleton-associated protein (Arc), also known as activity-regulated gene 3.1 (Arg3.1), is expressed mainly in excitatory neurons following neural activity to mediate functionally diverse actions [1]. In activity-dependent synaptic plasticity, such as long-term potentiation (LTP) and long-term depression, Arc protein is rapidly synthesized and degraded, indicating a transient and dynamic mode of action [2–5]. Stimulus-evoked expression of Arc is also required for memory, postnatal developmental plasticity of the visual cortex, and cognitive flexibility [3, 6–9]. These diverse functions are proposed to be mediated by distinct Arc-binding partner complexes in the postsynaptic compartment and the neuronal nucleus [10–14]. Arc protein is also capable of reversible self-association and formation of oligomers [15, 16]. Recently, Arc protein was shown to

✉ Yuta Ishizuka
yuta.ishizuka@med.kawasaki-m.ac.jp;
yishizuka1110@gmail.com

✉ Clive R. Bramham
clive.bramham@uib.no

¹ Department of Biomedicine, University of Bergen, Jonas Lies 91, 5009 Bergen, Norway

² Mohn Center for Research on the Brain, University of Bergen, Bergen, Norway

³ Faculty of Biochemistry and Molecular Medicine, University of Oulu, Oulu, Finland

⁴ Biocenter Oulu, University of Oulu, Oulu, Finland

⁵ Department of Pathophysiology and Metabolism, Kawasaki Medical School, 577 Matsushima, Kurashiki, Okayama 701-0192, Japan

self-assemble into spheroid particles resembling retroviral Gag capsids [17–19]. Arc capsids are incorporated in extracellular vesicles and are capable of transferring RNA cargo from donor cells to recipient cells [17, 18]. However, an integral understanding that accounts for Arc hub signaling and capsid function is lacking.

Arc is a flexible protein comprised of oppositely charged N- and C-terminal domains (NTD and CTD), flanking a central disordered hinge region [15]. Structural studies and predictions indicate an antiparallel coiled-coil structure of the NTD [20]. The NTD mediates binding of Arc to phospholipid membrane [20, 21]. NTD coil-2 harbors an oligomerization motif $^{113}\text{MHVWREV}^{119}$ that is critical for Arc self-association including formation of higher-order oligomers and capsids, but is not required for dimer formation [19]. The CTD is a tandem domain comprised of two lobes, the N- and C-lobes (NL and CL), homologous to the capsid domain of retroviral Gag polyprotein [14, 22]. The Arc CTD is important for higher-order oligomerization and formation of a double-shelled Arc capsid, secondary to NTD coil-2 mediated oligomerization [18, 19, 23]. In addition, the mammalian Arc NL has a unique hydrophobic peptide binding pocket that interacts with several postsynaptic proteins, including stargazin, guanylate kinase-associated protein (GKAP), Wiskott-Aldrich syndrome protein family member 1 (WAVE1), and GluN2A [14, 20, 22, 24]. Taken together, this suggests that interactions between domains regulates oligomerization and protein–protein interactions to determine Arc activity-state. However, tools that would allow labeling or functional manipulation of endogenous Arc in situ are lacking.

Single-domain antibody (sdAb), also known as variable domain of heavy chain (VHH) antibody or Nanobody® (Nb), are derived from the heavy chain antibody of *Camelidae* [25]. Nbs have unique properties relative to conventional antibodies that make them attractive for use as research tools and development of therapeutics [26]. Nbs are small (15 kDa), monovalent, chemically stable, and suitable for expression in mammalian cells as genetically encoded intrabodies. In addition, Nbs may bind hidden epitopes in small cavities that are not recognized by antibodies [27–31].

Here, we sought to develop and validate experimental applications for six anti-Arc nanobodies (ArcNbs: B5, B12, C11, D4, E5, and H11). ArcNbs fused to a small ALFA epitope [32] were successfully used for immunoblotting and immunoprecipitation of endogenous Arc. ArcNb E5 and H11 specifically recognized the Arc NL, while the other Nbs bound the segment containing the CL and C-terminal tail. Genetically encoded ArcNb fused to fluorescent mScarlet-I expressed efficiently in mammalian cells as intrabodies and allowed immunoprecipitation of intracellular Arc. The ArcNbs provide versatile tools for labeling, tracking, and

purifying native intracellular Arc, with further potential use as inhibitors of Arc CTD (capsid domain) specific functions.

Materials and Methods

Generation and Modifications of ArcNbs

Procedures for generation and modification of ArcNbs were conducted by NanoTag Biotechnologies GmbH (Göttingen, Germany) (Fig. 1). For detailed information on the purification, structural characterization, and binding of the untagged ArcNbs, see reference [33]. Briefly, two alpacas were immunized six times starting with purified recombinant human wild-type (WT) Arc (immunization 1 and 2), then a mixture of Arc WT and purified mutant rat Arc (Arc^{s113–119A}: in which residues of oligomerization motif were substituted to alanine) with increasing proportion of Arc^{s113–119A} (immunization 3–5), and finally with injection of Arc^{s113–119A} alone. A strong general immune response was confirmed using a serum-based ELISA in one of the animals. Total RNA was extracted from peripheral blood mononuclear cell (PBMC) preparations obtained from whole blood. cDNA encoding Nbs were reverse transcribed using a nested PCR that specifically amplifies the coding regions for IgG2 and IgG3 VHH fragments. The complete PCR product was cloned into a phagemid vector suitable for phage display followed by bio-panning with purified mutant Arc^{s113–119A} protein as antigen. Nb sequences extracted from phages binding to antigen were amplified by PCR and cloned into the screening vector. Ninety-six Nb clones were separately expressed in *E. coli*. and validated by ELISA using Arc^{s113–119A} as target protein. Six clones (B5, B12, C11, D4, E5, and H11) were chosen based on their sequences and ELISA-based binding evaluations.

To generate recombinant Nbs suitable for biochemical analyses, such as immunoblotting and immunoprecipitation, a small ALFA-epitope tag (SRLEEELRRRLTE) [32], which forms a stable α -helix on target protein, was added to the Nb C-terminus. For expressing ArcNbs as intrabody/chromobody, the Nb coding regions were subcloned from the bacterial expression vector into a mammalian expression vector harboring mScarlet-I (mSc) driven by the CMV promoter. We also subcloned the coding region of all ArcNbs into the AcGFP-N1 vector. AcGFP1-N1 was a gift from Michael Davidson (Addgene plasmid # 54,705; <http://n2t.net/addgene:54705>; RRID:Addgene 54705).

Purification of ALFA-Tagged ArcNbs

ALFA-tagged ArcNbs (ALFA-ArcNbs) were expressed in *E. coli* BL21 (DE3) cells and purified according to general methods [34] with minor modifications. Briefly, cells were

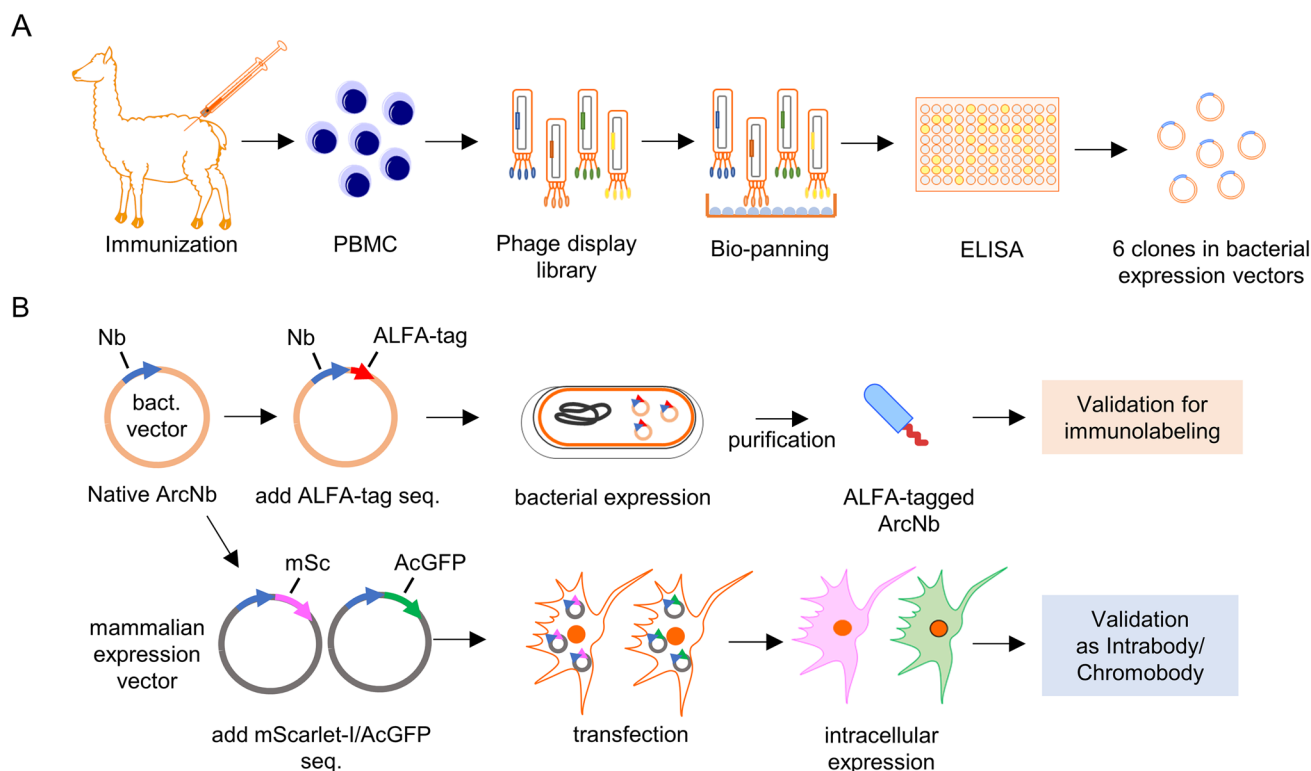


Fig. 1 Schematic of ArcNb generation and modifications. **A** Schematic of ArcNb generation pipeline. **B** Modifications of ArcNb for biochemical and immunolabeling, and applications as genetically encoded intrabodies. See Materials and Methods for detailed description

grown at 37 °C in LB medium overnight. The cultures were transferred to ZY5052 medium for auto-induction of protein expression at 37 °C for 4 h, then at 30 °C for 24 h. The cells were lysed in lysis/washing buffer containing 40 mM Hepes (pH 7.5), 100 mM NaCl, and 20 mM imidazole, by one freeze–thaw cycle followed by sonication. The lysates were centrifuged at 16,000 × *g* for 30 min at 4 °C and loaded onto a Ni–NTA resin. After washing resin with lysis/washing buffer, ALFA-ArcNbs were eluted by elution buffer containing 40 mM Hepes (pH 7.5), 100 mM NaCl, and 300 mM imidazole. His-tagged TEV protease was added to the eluate, and the samples were dialyzed against dialysis buffer containing 40 mM Hepes (pH 7.5), 100 mM NaCl and 1 mM dithiothreitol (DTT) overnight at 4 °C. The dialyzed samples were passed through a Ni–NTA resin again to remove the TEV protease and the cleaved His₁₀-tag. The Ni–NTA flow-through was loaded on a chromatography column (HiLoad® 16/60 Superdex® 75 PG, Cytiva, Marlborough, MA), equilibrated with degassed buffer (20 mM Tris–HCl pH 7.4, 150 mM NaCl). Size exclusion chromatography was run at 1 ml/min at 4 °C on an ÄKTA pure chromatography system (Cytiva). All ALFA-ArcNbs gave one major peak in the chromatogram. The protein size and purity were analyzed by SDS-PAGE, giving one strong Coomassie-stained band of the expected size (Fig. S1).

Animals, Electrophysiology, and Tissue Collection

For naive cortical tissue collection, adult male Sprague–Dawley rats were anesthetized using urethane (1.5 g/kg intraperitoneal) and decapitated before dissecting out cortical tissues. The tissues were kept in –80 °C until experiments. LTP in the dentate gyrus (DG) was induced as described [35]. Briefly, a bipolar stimulating electrode (7.9 mm posterior to the bregma, 4.2 mm lateral to the midline) and recording electrode (3.9 mm posterior to bregma, 2.3 mm lateral to midline) were inserted to stimulate medial perforant path fibers and record evoked field potentials in the dentate hilus, respectively. Test pulses were given every 30 s throughout the experiment except during the period of high-frequency stimulation (HFS). 20 min baseline recordings were acquired before three sessions of HFS with 5 min interval were given. Each session consisted of four, 400 Hz stimulus trains (8 pulses/train) and the interval between trains was 10 s. Changes in the field excitatory post-synaptic potential slope were expressed in percent of baseline to quantify the induction and maintenance of LTP. Two hours after HFS, rats were decapitated, and the dentate gyri were dissected out and stored at –80 °C for further use.

Cell Culture: Transfection and Pharmacological Stimulation

Human embryonic kidney 293FT (HEK293FT) and SH-SY5Y neuroblastoma cells were obtained from Thermo Fisher Scientific (Waltham, MA) and ATCC (Manassas, VA), respectively. Cells were maintained in Dulbecco's modified Eagle medium (DMEM/high-glucose, Sigma-Aldrich, St. Louis, MO) supplied with 10% FBS (Sigma-Aldrich) and 100 U/ml Penicillin-Streptomycin (Thermo Fisher Scientific) at 37 °C in a humidified incubator with 5% CO₂. HEK293FT cells were transfected using Lipofectamine™ 2000 Transfection Reagent (Thermo Fisher Scientific) according to the manufacturer's instructions. For induction of endogenous Arc expression, SH-SY5Y cells were stimulated with 100 μM carbachol (CCh) for 1 h at 37 °C in a humidified incubator with 5% CO₂ [36].

Antibodies

Primary antibodies are as follows: mouse anti-Arc (C-7) (Santa Cruz Biotechnology, Dallas, TX, Cat# sc-17839, RRID:AB_626696), rabbit anti-Arc (Synaptic Systems, Göttingen, Germany, Cat# 156 003, RRID:AB_887694), rabbit anti-GFP (Santa Cruz Biotechnology Cat# sc-8334, RRID:AB_641123), mouse anti-mCherry (Takara Bio, Siga, Japan, Cat# 632,543, RRID:AB_2307319), anti-ALFA HRP-coupled sdAb (NanoTag Biotechnologies, Cat# N1501-HRP). Secondary antibodies are as follows: Goat Anti-Mouse IgG, H & L Chain Antibody, Peroxidase Conjugated (Merck, Darmstadt, Germany, Cat# 401,253, RRID:AB_437779) and Goat Anti-Rabbit IgG, H & L Chain Specific Peroxidase Conjugate antibody (Merck Cat# 401,315, RRID:AB_2617117). Secondary antibodies for detecting immunoprecipitated proteins are as follows: Peroxidase AffiniPure Goat Anti-Mouse IgG, light chain specific (Jackson ImmunoResearch Labs, West Grove, PA, Cat# 115–035-174, RRID:AB_2338512) and Peroxidase IgG Fraction Monoclonal Mouse Anti-Rabbit IgG, light chain specific (Jackson ImmunoResearch Labs, Cat# 211–032-171, RRID:AB_2339149).

Electrophoresis and Immunoblotting

Native polyacrylamide gel electrophoresis (PAGE) was performed as described [37]. Briefly, different amounts of purified mutant Arc^{S113–119A} protein were dissolved in native sample buffer, then subjected to native PAGE using 4–15% Tris–Glycine acrylamide gels. SDS-PAGE was performed as described previously [38, 39]. Briefly, cultured cells and brain tissues were lysed and sonicated in RIPA buffer containing cOmplete™, EDTA-free Protease Inhibitor Cocktail Tablet (Sigma-Aldrich) and PhosSTOP™, Phosphatase

Inhibitor Cocktail Tablet (Sigma-Aldrich). After centrifugation, the supernatants were collected, and protein concentration was determined using the Micro BCA Protein Assay Kit (Thermo Fisher Scientific). Samples were mixed with 4X Laemmli sample buffer (Bio-Rad Laboratories, Inc., Hercules, CA) containing 50 mM DTT at final concentration, then boiled and subjected to SDS-PAGE. Separated proteins in the gel then were transferred to polyvinylidene difluoride membrane (Thermo Fisher Scientific). The membranes were incubated with the appropriate primary and secondary antibodies after incubation with 10% bovine serum albumin (BSA) in Tris-buffered saline with 0.05% Tween 20 (TBS-T) at room temperature for 1 h. For detecting Arc protein immunolabeled by ArcNb, anti-ALFA HRP-coupled sdAb was used instead of conventional secondary antibody. Peroxidase activity was detected using chemiluminescence reagent (Clarity Western ECL substrate, Bio-Rad Laboratories, Inc.) and visualized by an image analyzer using Image Lab™ Software (Gel Doc™ XR+, Bio-Rad Laboratories, Inc.). Figure presentations were performed using ImageJ/FIJI (RRID: RRID:SCR_002285).

Immunoprecipitation of Endogenous Arc Protein with ALFA-ArcNbs

Endogenous Arc immunoprecipitation was performed using ALFA-ArcNbs and ALFA SelectorST resin. In ALFA SelectorST, an ultra-high-affinity anti-ALFA Nb is covalently immobilized on agarose beads, allowing stringent purification of ALFA-tagged target proteins [32]. CCh-treated SH-SY5Y cells and DG tissue from HFS-treated rats were lysed in modified RIPA (M-RIPA) buffer (50 mM Tris–HCl pH 7.4, 150 mM NaCl, 1% NP-40, 0.25% sodium deoxycholate, 1 mM EDTA) supplemented with cOmplete™ (Sigma-Aldrich) and PhosSTOP™ (Sigma-Aldrich). First, 20 μl of ALFA SelectorST resin was washed twice in 1 ml M-RIPA buffer and centrifuged at 1,000×g for 1 min at 4 °C. Then, the resin was incubated with 2 μg of ALFA-ArcNb H11 for 1 h at 4 °C with head-over-tail rotation. Following washing, the ALFA-ArcNb H11 and selector resin complex was incubated with lysates for 30 min at room temperature. After washing resin, the samples were mixed with 2X Laemmli sample buffer containing 100 mM DTT at final concentration and denatured by boiling at 95 °C for 5 min. The supernatants were subjected to SDS-PAGE followed by immunoblotting for analyzing precipitated complexes.

Fluorescence Cell Imaging

Preparation of coverslips for cell imaging was performed according to previously described methods [39]. HEK293FT cells seeded on coverslips in 12-well plates were transfected with mSc-ArcNb expression vectors according to the

manufacturer's instructions. Transfected cells were fixed with 4% paraformaldehyde in 0.1 M phosphate buffer (pH 7.4) for 20 min at room temperature. After washing coverslips with phosphate-buffered saline (PBS, pH 7.4), the coverslips were mounted in Prolong™ Diamond Antifade Mountant with DAPI (Thermo Fisher Scientific). Fluorescence imaging was performed on an AxioImager Z1 microscope (Carl Zeiss AG, Oberkochen, Germany). Transfected cells were imaged using Plan-ApoChromat 20x/0.75 NA (Carl Zeiss AG), EC plan Neofluar 40x/1.30 Oil M27 (Carl Zeiss AG) objectives, and AxioCam 503 mono digital camera controlled by ZEN pro software (Carl Zeiss AG). The captured fluorescence images were analyzed using MetaMorph® imaging software (Molecular Devices, San Jose, CA) and ImageJ/Fiji.

Co-Immunoprecipitation

HEK293FT cells were co-transfected with plasmids expressing mSc-ArcNb H11 (mSc-H11) and an mTurquoise2 (mTq2)-tagged Arc construct. mTq2 was N-terminally fused to 1) Arc full-length (FL), 2) N-terminal region (NTR 1–140), 3) linker (135–216), 4) C-terminal region (CTR 208–396), 5) N-lobe (NL 208–277), or 6) C-lobe + C-terminal tail (CL + tail 278–396). Transfected cells were lysed in M-RIPA buffer. First, 2 µg of normal rabbit IgG (Merck, Cat# 12–370, RRID:AB_145841), anti-mCherry (mCh) antibody against mSc-H11, or anti-Arc rabbit polyclonal antibody were absorbed to Protein G Sepharose 4 Fast Flow (Cytiva) for 1 h at room temperature. Then, antibody/bead complexes were mixed with the cell lysates overnight at 4 °C for co-immunoprecipitation (co-IP). The sepharose beads were washed four times with M-RIPA buffer and resuspended in 2X Laemmli sample buffer containing 100 mM DTT before denaturing at 95 °C for 5 min. The supernatants were subjected to SDS-PAGE followed by immunoblot analysis.

Results

ALFA-ArcNbs Recognize Purified Recombinant Arc and Endogenous Arc Protein

Two alpacas were immunized with a combination of purified recombinant human WT Arc and rat mutant Arc^{s113–119A} [33]. WT Arc self-associates and oligomerizes in vitro [15, 16]. We have recently shown that amino acid residues 113–119 are critical for high-order oligomerization [19]. Interestingly, the substitution mutant protein Arc^{s113–119A} failed to form high-order oligomers or capsids. A mixture of WT and Arc^{s113–119A} mutant protein was used as an antigen cocktail because oligomerization of WT Arc protein might

lead to epitope masking, preventing a full immune response. Following a bio-panning assay using Arc^{s113–119A} as target, 96 clones were expressed and evaluated by ELISA using mutant Arc^{s113–119A} as an antigen. Six clones (B5, B12, C11, D4, E5, and H11) representing different clonal lines were chosen based on their sequences and ELISA-based binding to purified Arc^{s113–119A}.

Firstly, we examined whether ALFA-ArcNbs have ability to detect purified recombinant Arc and endogenous Arc from rat cortical lysates. In immunoblot assays, ALFA-ArcNb bound to Arc was detected by using anti-ALFA HRP-coupled sdAb. All six ArcNbs bound to purified Arc^{s113–119A} both in native and denaturing conditions (Fig. S2). On native PAGE gels (Fig. S2A), several immunoreactive bands were detected as lower-order oligomeric forms. In the denaturing condition on SDS-PAGE (Fig. S2B), only one prominent immunoreactive band was detected around 50 kDa, corresponding to Arc monomer. Also, immunoblotting performed in cortical lysates from naïve rats showed that all ArcNbs detect endogenous Arc as a single band (~50 kDa) consistent with conventional anti-Arc antibodies (Fig. 2A). We then tested whether ALFA-ArcNbs are suitable for immunoprecipitation of endogenous, stimulus-induced Arc. CCh treatment of SH-SY5Y cells and HFS-induced LTP in the rat DG in vivo are both associated with enhanced Arc expression [3, 36, 40]. SH-SY5Y cells were stimulated with 100 µM CCh for 1 h and subjected to immunoprecipitation using ALFA-ArcNb H11 and ALFA SelectorST resin, followed by SDS-PAGE and immunoblotting using anti-Arc rabbit polyclonal antibody. CCh treatment induced a prominent increase in Arc expression in whole lysate, shown as input samples in figures, relative to untreated cells (Fig. 2B, closed arrowhead), and immunoprecipitation using ALFA-ArcNb H11 massively enriched for Arc (Fig. 2B, opened arrowhead). Similarly, HFS resulted in ipsilateral enhancement of Arc expression in the DG (Fig. 2C, closed arrowhead), which was strongly enriched in the immunoprecipitation (Fig. 2C, opened arrowhead). These results validate all ALFA-ArcNbs for immunoblotting and ALFA-ArcNb H11 for immunoprecipitation of endogenous Arc.

ALFA-ArcNbs E5 and H11 Specifically Bind to Arc-NL

Next, we performed epitope mapping by expressing Arc-FL or truncation mutants in HEK293FT cells, followed by SDS-PAGE and immunoblot analysis with the six ALFA-ArcNbs. Cells were first transfected with mTq2-Arc 1) full-length (FL), 2) N-terminal region (NTR 1–140), 3) linker region (linker 135–216), 4) C-terminal region (CTR 208–396) (Fig. 3A). All ArcNbs detected Arc FL and CTR, but none bound to the NTR or linker region fragments. To further specify the region of binding, cells were transfected with mTq2-Arc-NL (208–277, lane 5) or CL + tail (278–396, lane

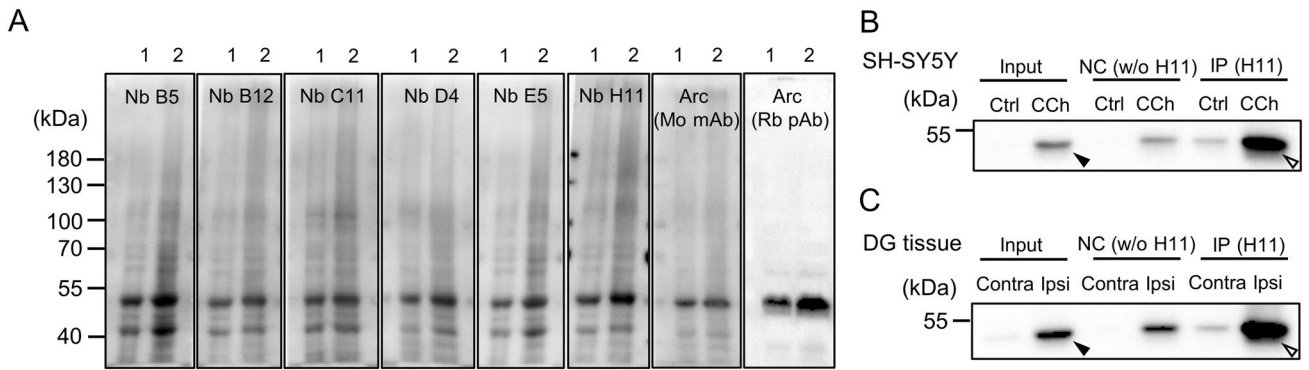


Fig. 2 ALFA-ArcNbs for immunoblotting and immunoprecipitation analysis of endogenous Arc. **A** Rat cortical tissues were lysed in RIPA buffer. Different amounts of lysates were subject to SDS-PAGE followed by immunoblotting using ALFA-ArcNbs (B5, B12, C11, D4, E5, and H11) and conventional anti-Arc antibodies as reference. Immunoreactive bands corresponding to Arc were detected around 50 kDa (lane 1, 30 µg; lane 2, 60 µg). **B** CCh (100 µM, 1 h)-treated SH-SY5Y cells were lysed and subjected to immunoprecipitation using ALFA-ArcNb H11 and ALFA Selector™ followed by

SDS-PAGE and immunoblotting using anti-Arc antibody. NC, negative control (ALFA SelectorST resin without ALFA-ArcNb H11). **C** HFS was applied unilaterally to the perforant path input to the dentate gyrus (DG) of anesthetized rats to induce LTP. At 2 h post-HFS, DG tissue was collected from the ipsilateral (Ipsi) and contralateral (Contra) DG, and immunoprecipitation analysis was performed as described in panel B. Strong enrichment of Arc was obtained upon addition of ALFA-ArcNb H11 (open arrows). The signal in negative control is attributed to non-specific Arc binding to agarose resin

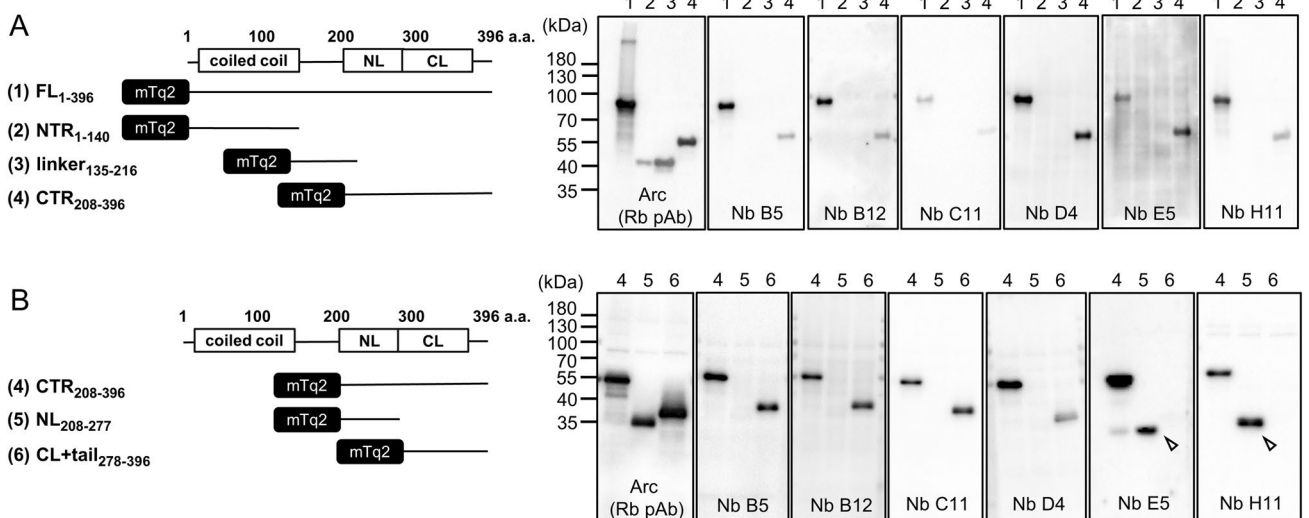


Fig. 3 Epitope mapping of ArcNbs. **A** HEK293FT cells were transfected with mTq2-Arc-FL (residues 1–396) and truncation mutants expressing the Arc NTR (1–140), linker (135–216), or CTR (208–396). **B** Cells were transfected with mTq2-truncation mutants expressing the Arc CTR, isolated NL, or CL+tail. Cell lysates were

subjected to SDS-PAGE followed by immunoblotting using ALFA-ArcNbs and anti-Arc antibody. 1, FL (residues 1–396); 2, NTR (residues 1–140); 3, linker region (residues 135–216); 4, CTR (residues 208–396); 5, NL (residues 208–277); 6, CL+tail (residues 278–396)

6), then subjected to immunoblotting. Intriguingly, ArcNbs E5 and H11 specifically bound to NL (Fig. 3B, open arrowheads), while all other Nbs (B5, B12, C11, and D4) bound to the CL+tail region (Fig. 3B).

Expression of mScarlet-I-Tagged and AcGFP-Tagged ArcNbs as Intrabodies in HEK293FT Cells

We tested intracellular expression of ArcNbs in mammalian cells as genetically encoded intrabodies. HEK293FT cells were transfected with mSc-ArcNb expression vectors, then subjected to SDS-PAGE followed by immunoblotting using anti-mCh antibody to detect mSc. Expression of mSc-ArcNbs was confirmed by immunoblotting (Fig. 4A) and

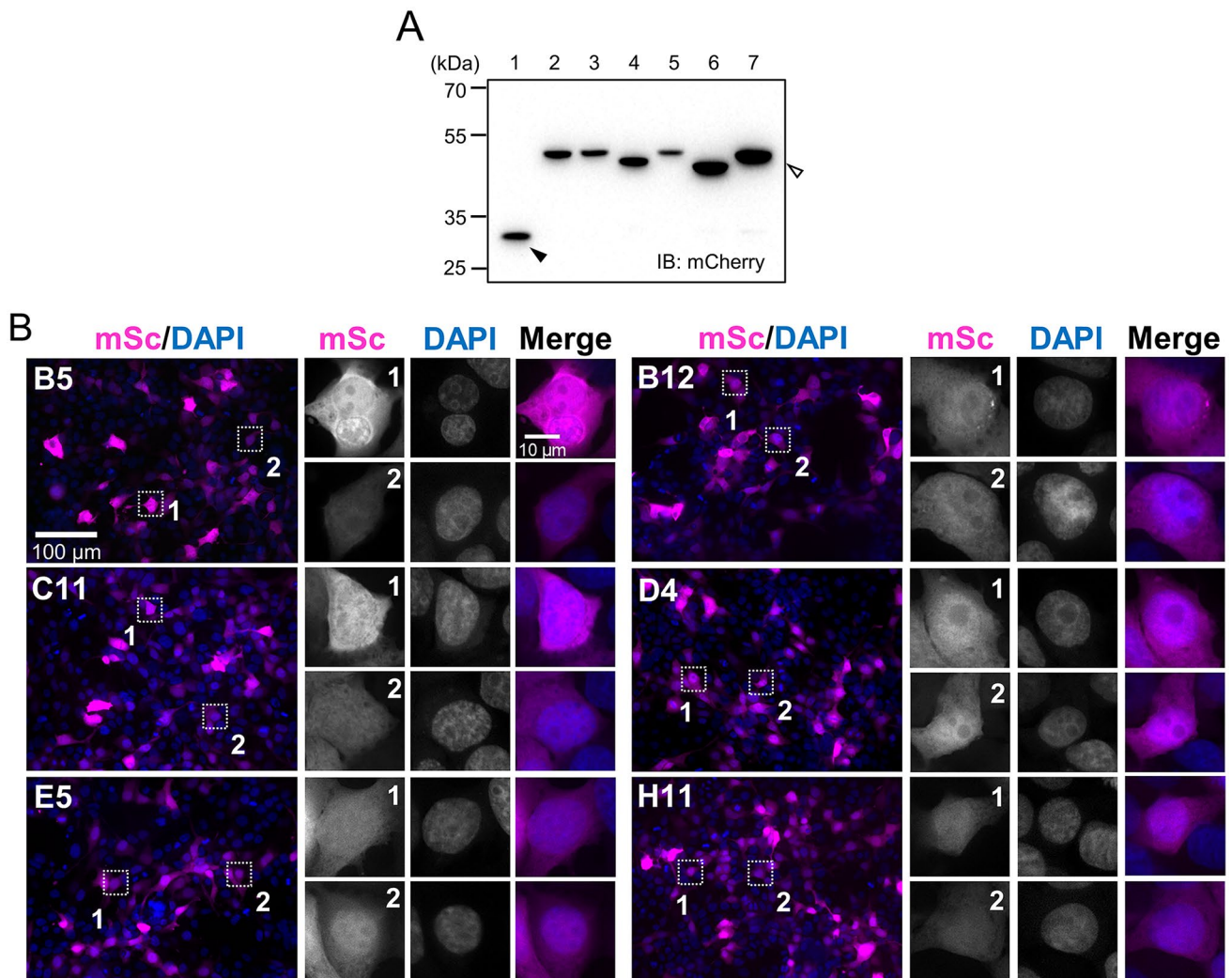


Fig. 4 mSc-ArcNb expression in HEK293FT cells as intrabody. **A** HEK293FT cells were transfected with mSc control vector (Mock, closed arrowhead) or mSc-ArcNb expression vectors (open arrowhead). Cell lysates were subjected to SDS-PAGE followed by immunoblotting using anti-mCh antibody against mSc-tag. Lane 1, Mock;

2, B5; 3, B12; 4, C11; 5, D4; 6, E5; 7, H11. **B** HEK293FT cells transfected with mSc-ArcNbs were fixed and imaged by fluorescence microscopy. Left, low magnification images with two representative cells marked with a stippled square. Right, high magnification images of the marked cells

fluorescence microscopy (Fig. 4B). All six mSc-ArcNbs exhibited uniformly bright cytoplasmic and nucleoplasmic fluorescence without selective accumulation in subcellular compartments, formation of aggregates, or signs of morphological abnormalities. We also assessed the expression pattern of AcGFP-ArcNbs (Fig. S3A). AcGFP fused to either E5, C11, or H11 showed uniform fluorescence similar to the corresponding mSc-ArcNbs. However, in contrast to the mSc-ArcNbs, three of the AcGFP-ArcNbs (B5, B12, and D4) showed strong accumulation and aggregation in the nucleus (Fig. S3B). These results indicate that all mSc-ArcNbs and several AcGFP-ArcNbs can be expressed as intrabodies without aggregation or deleterious effects.

mScarlet-I-Tagged ArcNb H11 Intrabody Specifically Binds the N-lobe and Enables Immunoprecipitation of Intracellular Arc

We examined whether ArcNb, when expressed as intrabody, can bind intracellular Arc. We focused this analysis on ArcNb H11, which efficiently immunoprecipitated endogenous Arc (Fig. 2) and selectively bound the NL in the epitope mapping analysis (Fig. 3). HEK293FT cells were co-expressed with mTq2-Arc (FL) together with mSc-H11, then subjected to co-IP assays using either anti-mCh or rabbit anti-Arc polyclonal antibodies to immunoprecipitate the Arc/ArcNb complex (design illustrated in Fig. 5A). As expected, mSc-H11 was immunoprecipitated with anti-mCh antibody (Fig. 5B, closed arrowhead). Importantly,

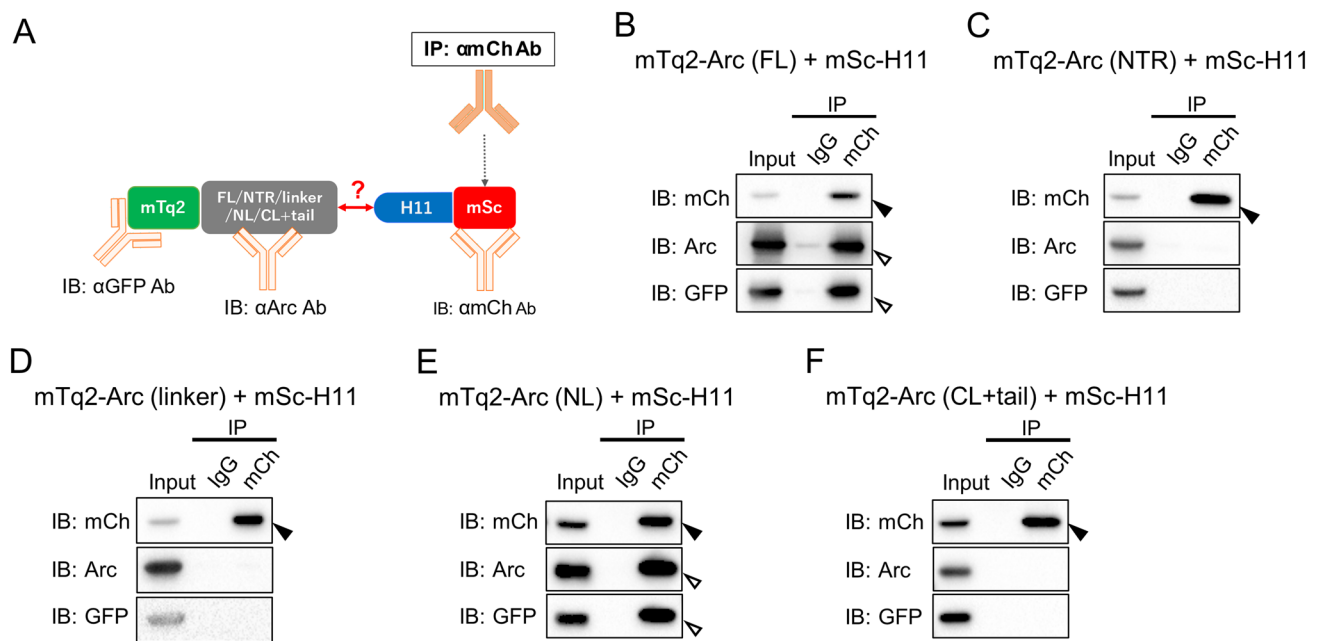


Fig. 5 Co-immunoprecipitation of intracellular Arc full-length and isolated N-lobe using mSc-H11 intrabody. **A** Schema of co-IP assay. **B–F** co-IP assay. HEK293FT cells were co-transfected with mTq2-Arc-FL (**B**), NTR (**C**), linker region (**D**), NL (**E**), or CL + tail (**F**) and mSc-H11 constructs. Cell lysates were then subjected to co-IP assay

using anti-mCh antibody. Following SDS-PAGE, immunoprecipitants were probed using anti-mCh, anti-Arc, and anti-GFP antibodies. Closed and open arrowheads indicate immunoprecipitated mSc-H11 and co-immunoprecipitated Arc variants, respectively

mSc-H11 in complex with mTq2-Arc (FL) was co-immunoprecipitated by anti-mCh antibody, as detected by both anti-Arc and anti-GFP antibodies (Fig. 5B, opened arrowheads). In cells co-transfected with mTq2-Arc NTR or mTq2-Arc linker, no interaction of mSc-H11 with these Arc regions was detected, although successful immunoprecipitation of mSc-H11 with anti-mCh antibody was confirmed (Fig. 5C, D, closed arrowheads). To further assess the intracellular specificity of binding, cells were co-transfected with mTq2-Arc NL or mTq2-Arc CL + tail together with mSc-H11. We found that H11 forms an intracellular complex with Arc NL (Fig. 5E, opened arrowhead) but not with the CL + tail (Fig. 5F). We also did a reverse co-IP assay using rabbit anti-Arc polyclonal antibody (Fig. S4) and found that mSc-H11 was co-immunoprecipitated with Arc FL and NL (Figs. S4B and E, opened arrowheads), but not with Arc NTR, linker, or CL + tail (Figs. S4C, D and F). Taken together, we conclude that ArcNb H11 expressed as intrabody specifically binds the Arc NL and can be used to affinity-purify intracellular full-length Arc.

Discussion

We developed and validated the first ArcNbs [33] as new tools for probing Arc expression and function. For biochemical analyses, the small ALFA epitope tag was fused to the

C-terminus of ArcNbs [32]. All clones of ALFA-ArcNbs detected purified recombinant Arc protein and endogenous Arc protein from rat brain tissues (Figs. S2 and 2A). We show that ALFA-ArcNbs combined with anti-ALFA HRP-coupled sdAbs can be used for immunoblotting of Arc protein in the same manner as conventional anti-Arc antibodies. All six ArcNbs bound selectively to the Arc CTR. Nbs E5 and H11 bound to the CTD NL, while the remaining four Nbs bound to the segment containing the CL and C-terminal tail (Fig. 3). The fact that none of the Nbs generated in alpaca bound to the NTR is surprising and might be due to cleavage and selective degradation of the NTR after injection, or to low immunogenicity of the region.

Using a mammalian expression vector harboring mSc or AcGFP fluorescent proteins, we showed that all ArcNbs are suitable for applications as genetically encoded chromobodies (Figs. 4A and S3B). mSc is a bright monomeric red fluorescent protein [41, 42]. AcGFP1 is a monomeric green fluorescent protein, obtained from *Aequorea coerule-scens*, with similar spectral properties to EGFP. Despite 94% amino acid sequence similarity and equivalent brightness, AcGFP1 is superior to EGFP for fusion applications because it is monomeric [43] unlike EGFP that forms dimers [44, 45]. Although all mSc-ArcNbs showed uniform cytosolic and nuclear expression, three of the AcGFP-ArcNbs (B5, B12 and D4) aggregated in the nucleus (Fig. S3B). Further

experiments are needed to understand the mechanism of nuclear aggregation of these AcGFP-ArcNbs.

In the parallel study on the generation and structural characterization of ArcNbs [33], purified untagged Nbs served as chaperones for crystallization of mammalian Arc. Atomic structures were obtained of ArcNb H11 and C11 bound to NL and CL, respectively [33]. Moreover, the complementarity determining region 3 (CDR3) of ArcNb H11 was shown to bind inside the hydrophobic pocket of the NL [33]. The CDR3 in ArcNb H11 harbors an amino acid sequence that corresponds to the identified NL ligand binding motif [14, 20]. Isothermal titration calorimetry showed that ArcNb H11 binds with high affinity (1 nM K_d) and competitively displaces stargazin, an auxiliary subunit of AMPA-type glutamate receptors, which has the highest binding affinity (34.9 nM) of the known Arc NL ligands [33]. The present work shows that genetically encoded ArcNb H11 expressed in mammalian cells binds specifically to the NL and enables co-IP of intracellular Arc (Figs. 5 and S4). ArcNb H11 also enabled efficient immunoprecipitation of endogenous Arc synthesized during the maintenance phase of LTP in the rat DG *in vivo* (Fig. 2). Taken together, these findings make ArcNb H11 attractive as a high-affinity binder for labeling and tracking Arc inside cells, and a candidate competitive inhibitor of Arc function, by blocking protein–protein interaction and signaling mediated by the N-lobe *in vivo*. Ideally, Nbs used for intracellular tracking of Arc would not interfere with protein activity or oligomerization. These features need to be characterized for each of the nanobodies.

ArcNbs B5, B12, C11, and D4 bound to the region encompassing the Arc CL and C-terminal tail (Fig. 3B). However, specific association with the CL domain is likely, as recombinant purified ArcNbs bound to the isolated CTD [33]. Furthermore, crystal structure analysis of untagged ArcNb C11 in complex with the CTD demonstrated binding to the CL in a region that encompasses a conserved retroviral capsid dimerization motif [14, 23, 33]. Thus, ArcNb C11 is of interest as a potential inhibitor of CL-mediated interactions in the context of full-length Arc oligomerization, and eventual capsid assembly. Although CL is structurally homologous to NL [14], there is no evidence of similar peptide ligand binding [20, 24].

In conclusion, we developed two lines of ArcNbs: one (clones E5 and H11) for binding to NL and another (clones B5, B12, C11, and D4) for binding the CL and C-terminal region. These new tools open a range of possibilities, including expression of intrabodies for labelling and tracking endogenous Arc in live-cell imaging experiments and for biochemical isolation of native Arc complexes. Given their stable expression and high-affinity binding, it will be important in future work to evaluate ArcNbs as genetically encoded inhibitors of Arc NL signaling and oligomerization in neurons. ArcNbs can be used and further developed to

elucidate Arc domain-specific mechanisms and functions in synaptic plasticity. Viral vector mediated expression of ArcNbs may enable dissection of function in specific cell types and circuits *in vivo*. Furthermore, the recombinant ALFA-ArcNbs may be useful in efforts to detect oligomers and isolate intact capsids from brain tissue and other sources.

Supplementary Information The online version contains supplementary material available at <https://doi.org/10.1007/s11064-022-03573-5>.

Acknowledgements We would like to thank The Laboratory Animal Facility of University of Bergen for maintaining experimental animals. This work was supported by a Research Council of Norway Toppforsk grant (249951) to CRB.

Author Contributions YI: Conceptualization, Methodology, Validation, Investigation, Resources, Data Curation, Writing – Original Draft, Visualization, Supervision, Project administration. TFM: Validation, Investigation, Data Curation, Writing – Review & Editing. RB: Investigation, Validation. JX: Investigation, Resources. EIH: Resources. SM: Resources, PK: Conceptualization, Resources, Project administration. Supervision, Funding acquisition. CRB: Conceptualization, Writing – Review & Editing, Supervision, Methodology, Resources, Data Curation, Funding acquisition, Project administration.

Funding Open access funding provided by University of Bergen (incl Haukeland University Hospital).

Data Availability The datasets generated and analyzed during the current study are available from the corresponding authors on reasonable request.

Declarations

Conflict of interest The authors declare no competing interest.

Ethical Approval All experimental procedures were approved by the Norwegian National Research Ethics Committee in compliance with EU Directive 2010/63/EU, ARRIVE guidelines. All methods were carried out in accordance with relevant guidelines and regulations. Persons involved in the animal experiments have approved Federation of Laboratory and Animal Science Associations (FELASA) C course certificates and training.

Consent for Publication All authors reviewed and approved the manuscript.

Open Access This article is licensed under a Creative Commons Attribution 4.0 International License, which permits use, sharing, adaptation, distribution and reproduction in any medium or format, as long as you give appropriate credit to the original author(s) and the source, provide a link to the Creative Commons licence, and indicate if changes were made. The images or other third party material in this article are included in the article's Creative Commons licence, unless indicated otherwise in a credit line to the material. If material is not included in the article's Creative Commons licence and your intended use is not permitted by statutory regulation or exceeds the permitted use, you will need to obtain permission directly from the copyright holder. To view a copy of this licence, visit <http://creativecommons.org/licenses/by/4.0/>.

References

- Nikolaïenko O, Patil S, Eriksen MS, Bramham CR (2018) Arc protein: a flexible hub for synaptic plasticity and cognition. *Semin Cell Dev Biol* 77:33–42. <https://doi.org/10.1016/j.semcdb.2017.09.006>
- Bramham CR, Alme MN, Bittins M, Kuipers SD, Nair RR, Pai B, Panja D, Schubert M, Soule J, Tiron A, Wibrand K (2010) The Arc of synaptic memory. *Exp Brain Res* 200:125–140. <https://doi.org/10.1007/s00221-009-1959-2>
- Messaoudi E, Kanhema T, Soule J, Tiron A, Dageyte G, da Silva B, Bramham CR (2007) Sustained Arc/Arg3.1 synthesis controls long-term potentiation consolidation through regulation of local actin polymerization in the dentate gyrus in vivo. *J Neurosci* 27:10445–10455. <https://doi.org/10.1523/JNEUROSCI.2883-07.2007>
- Zhang H, Bramham CR (2021) Arc/Arg3.1 function in long-term synaptic plasticity: Emerging mechanisms and unresolved issues. *Eur J Neurosci* 54:6696–6712. <https://doi.org/10.1111/ejn.14958>
- Waung MW, Pfeiffer BE, Nosyreva ED, Ronesi JA, Huber KM (2008) Rapid translation of Arc/Arg3.1 selectively mediates mGluR-dependent LTD through persistent increases in AMPAR endocytosis rate. *Neuron* 59:84–97. <https://doi.org/10.1016/j.neuron.2008.05.014>
- Gao X, Castro-Gomez S, Grendel J, Graf S, Susens U, Binkle L, Mensching D, Isbrandt D, Kuhl D, Ohana O (2018) Arc/Arg3.1 mediates a critical period for spatial learning and hippocampal networks. *Proc Natl Acad Sci U S A* 115:12531–12536. <https://doi.org/10.1073/pnas.1810125115>
- Guzowski JF, Lyford GL, Stevenson GD, Houston FP, McGaugh JL, Worley PF, Barnes CA (2000) Inhibition of activity-dependent arc protein expression in the rat hippocampus impairs the maintenance of long-term potentiation and the consolidation of long-term memory. *J Neurosci* 20:3993–4001
- Jenks KR, Kim T, Pastuzyn ED, Okuno H, Taibi AV, Bito H, Bear MF, Shepherd JD (2017) Arc restores juvenile plasticity in adult mouse visual cortex. *Proc Natl Acad Sci U S A* 114:9182–9187. <https://doi.org/10.1073/pnas.1700866114>
- Plath N, Ohana O, Dammermann B, Errington ML, Schmitz D, Gross C, Mao X, Engelsberg A, Mahlke C, Welzl H, Kobalz U, Stawrakakis A, Fernandez E, Waltereit R, Bick-Sander A, Therstappen E, Cooke SF, Blanquet V, Wurst W, Salmen B, Bosl MR, Lipp HP, Grant SG, Bliss TV, Wolfer DP, Kuhl D (2006) Arc/Arg3.1 is essential for the consolidation of synaptic plasticity and memories. *Neuron* 52:437–444. <https://doi.org/10.1016/j.neuron.2006.08.024>
- Zhang H, Bramham CR (2020) Bidirectional dysregulation of AMPA receptor-mediated synaptic transmission and plasticity in brain disorders. *Front Synaptic Neurosci* 12:26. <https://doi.org/10.3389/fnsyn.2020.00026>
- Chowdhury S, Shepherd JD, Okuno H, Lyford G, Petralia RS, Plath N, Kuhl D, Huganir RL, Worley PF (2006) Arc/Arg3.1 interacts with the endocytic machinery to regulate AMPA receptor trafficking. *Neuron* 52:445–459. <https://doi.org/10.1016/j.neuron.2006.08.033>
- Okuno H, Akashi K, Ishii Y, Yagishita-Kyo N, Suzuki K, Nonaka M, Kawashima T, Fujii H, Takemoto-Kimura S, Abe M, Natsume R, Chowdhury S, Sakimura K, Worley PF, Bito H (2012) Inverse synaptic tagging of inactive synapses via dynamic interaction of Arc/Arg3.1 with CaMKIIbeta. *Cell* 149:886–898. <https://doi.org/10.1016/j.cell.2012.02.062>
- Nair RR, Patil S, Tiron A, Kanhema T, Panja D, Schiro L, Parobczak K, Wilczynski G, Bramham CR (2017) Dynamic Arc sumoylation and selective interaction with F-Actin-binding protein Drebrin A in LTP consolidation in vivo. *Front Synaptic Neurosci* 9:8. <https://doi.org/10.3389/fnsyn.2017.00008>
- Zhang W, Wu J, Ward MD, Yang S, Chuang YA, Xiao M, Li R, Leahy DJ, Worley PF (2015) Structural basis of arc binding to synaptic proteins: implications for cognitive disease. *Neuron* 86:490–500. <https://doi.org/10.1016/j.neuron.2015.03.030>
- Myrum C, Baumann A, Bustad HJ, Flydal MI, Mariaule V, Alvira S, Cuellar J, Haavik J, Soule J, Valpuesta JM, Marquez JA, Martinez A, Bramham CR (2015) Arc is a flexible modular protein capable of reversible self-oligomerization. *Biochem J* 468:145–158. <https://doi.org/10.1042/BJ20141446>
- Byers CE, Barylko B, Ross JA, Southworth DR, James NG, Taylor CAT, Wang L, Collins KA, Estrada A, Waung M, Tassin TC, Huber KM, Jameson DM, Albanesi JP (2015) Enhancement of dynamin polymerization and GTPase activity by Arc/Arg3.1. *Biochim Biophys Acta* 1850:1310–1318
- Ashley J, Cordy B, Lucia D, Fradkin LG, Budnik V, Thomson T (2018) Retrovirus-like gag protein Arc1 binds RNA and traffics across synaptic boutons. *Cell* 172(262–274):e211. <https://doi.org/10.1016/j.cell.2017.12.022>
- Pastuzyn ED, Day CE, Kearns RB, Kyrke-Smith M, Taibi AV, McCormick J, Yoder N, Belnap DM, Erlendsson S, Morado DR, Briggs JAG, Feschotte C, Shepherd JD (2018) The neuronal gene Arc encodes a repurposed retrotransposon gag protein that mediates intercellular RNA transfer. *Cell* 172(275–288):e218. <https://doi.org/10.1016/j.cell.2017.12.024>
- Eriksen MS, Nikolaïenko O, Hallin EI, Grodem S, Bustad HJ, Flydal MI, Merski I, Hosokawa T, Lascu D, Akerkar S, Cuellar J, Chambers JJ, O’Connell R, Muruganandam G, Loris R, Touma C, Kanhema T, Hayashi Y, Stratton MM, Valpuesta JM, Kursula P, Martinez A, Bramham CR (2021) Arc self-association and formation of virus-like capsids are mediated by an N-terminal helical coil motif. *FEBS J* 288:2930–2955. <https://doi.org/10.1111/febs.15618>
- Hallin EI, Eriksen MS, Baryshnikov S, Nikolaïenko O, Grodem S, Hosokawa T, Hayashi Y, Bramham CR, Kursula P (2018) Structure of monomeric full-length ARC sheds light on molecular flexibility, protein interactions, and functional modalities. *J Neurochem* 147:323–343. <https://doi.org/10.1111/jnc.14556>
- Barylko B, Wilkerson JR, Cavalier SH, Binns DD, James NG, Jameson DM, Huber KM, Albanesi JP (2018) Palmitoylation and membrane binding of Arc/Arg3.1: a potential role in synaptic depression. *Biochemistry* 57:520–524. <https://doi.org/10.1021/acs.biochem.7b00959>
- Nielsen LD, Pedersen CP, Erlendsson S, Teilum K (2019) The Capsid Domain of Arc Changes Its Oligomerization Propensity through Direct Interaction with the NMDA Receptor. *Structure* 27(1071–1081):e1075. <https://doi.org/10.1016/j.str.2019.04.001>
- Zhang W, Chuang YA, Na Y, Ye Z, Yang L, Lin R, Zhou J, Wu J, Qiu J, Savonenko A, Leahy DJ, Huganir R, Linden DJ, Worley PF (2019) Arc Oligomerization is regulated by CaMKII phosphorylation of the gag domain: an essential mechanism for plasticity and memory formation. *Mol Cell* 75(13–25):e15. <https://doi.org/10.1016/j.molcel.2019.05.004>
- Hallin EI, Bramham CR, Kursula P (2021) Structural properties and peptide ligand binding of the capsid homology domains of human Arc. *Biochem Biophys Rep* 26:100975. <https://doi.org/10.1016/j.bbrep.2021.100975>
- Hamers-Casterman C, Atarhouch T, Muyldermans S, Robinson G, Hamers C, Songa EB, Bendahman N, Hamers R (1993) Naturally occurring antibodies devoid of light chains. *Nature* 363:446–448. <https://doi.org/10.1038/363446a0>
- Steele S, Vandenbroucke RE, Libert C (2016) Nanobodies as therapeutics: big opportunities for small antibodies. *Drug Discov Today* 21:1076–1113. <https://doi.org/10.1016/j.drudis.2016.04.003>

27. Li T, Vandesquille M, Koukouli F, Dudeffant C, Youssef I, Lenormand P, Ganneau C, Maskos U, Czech C, Grueninger F, Duyckaerts C, Dhenain M, Bay S, Delatour B, Lafaye P (2016) Camelid single-domain antibodies: A versatile tool for in vivo imaging of extracellular and intracellular brain targets. *J Control Release* 243:1–10. <https://doi.org/10.1016/j.jconrel.2016.09.019>
28. Dong JX, Lee Y, Kirmiz M, Palacio S, Dumitras C, Moreno CM, Sando R, Santana LF, Sudhof TC, Gong B, Murray KD, Trimmer JS (2019) A toolbox of nanobodies developed and validated for use as intrabodies and nanoscale immunolabels in mammalian brain neurons. *Elife*. <https://doi.org/10.7554/eLife.48750>
29. Beghein E, Gettemans J (2017) Nanobody technology: a versatile toolkit for microscopic imaging, protein-protein interaction analysis, and protein function exploration. *Front Immunol* 8:771. <https://doi.org/10.3389/fimmu.2017.00771>
30. Gerdes C, Waal N, Offner T, Fornasiero EF, Wender N, Verbarq H, Manzini I, Trenkwalder C, Mollenhauer B, Strohaber T, Zweckstetter M, Becker S, Rizzoli SO, Basmanav FB, Opazo F (2020) A nanobody-based fluorescent reporter reveals human alpha-synuclein in the cell cytosol. *Nat Commun* 11:2729. <https://doi.org/10.1038/s41467-020-16575-0>
31. Muylldermsans S (2021) A guide to: generation and design of nanobodies. *FEBS J* 288:2084–2102. <https://doi.org/10.1111/febs.15515>
32. Gotzke H, Kilisch M, Martinez-Carranza M, Sograte-Idrissi S, Rajavel A, Schlichthaerle T, Engels N, Jungmann R, Stenmark P, Opazo F, Frey S (2019) The ALFA-tag is a highly versatile tool for nanobody-based bioscience applications. *Nat Commun* 10:4403. <https://doi.org/10.1038/s41467-019-12301-7>
33. Markússon S, Hallin EI, Bustad HJ, Raasakka A, Xu J, Muruganandam G, Loris R, Martinez A, Bramham CR, Kursula P (2021) High-affinity nanobodies as tools for structural and functional studies on mammalian Arc. *bioRxiv*:2021.2012.2016.472929. <https://doi.org/10.1101/2021.12.16.472929>
34. Hallin EI, Markússon S, Bottger L, Torda AE, Bramham CR, Kursula P (2021) Crystal and solution structures reveal oligomerization of individual capsid homology domains of *Drosophila* Arc. *PLoS ONE* 16:e0251459. <https://doi.org/10.1371/journal.pone.0251459>
35. Panja D, Bramham CR (2017) BDNF Function in Long-Term Synaptic Plasticity in the Dentate Gyrus In Vivo: Methods for Local Drug Delivery and Biochemical Analysis of Translation. In: Duarte C, Tongiorgi E (eds) *Brain-Derived Neurotrophic Factor (BDNF)*. Humana, New York, pp 241–256
36. Soule J, Alme M, Myrum C, Schubert M, Kanhema T, Bramham CR (2012) Balancing Arc synthesis, mRNA decay, and proteasomal degradation: maximal protein expression triggered by rapid eye movement sleep-like bursts of muscarinic cholinergic receptor stimulation. *J Biol Chem* 287:22354–22366. <https://doi.org/10.1074/jbc.M112.376491>
37. Drab T, Kracmerova J, Ticha I, Hanzlikova E, Ticha M, Liberda J (2011) Native polyacrylamide electrophoresis in the presence of Ponceau Red to study oligomeric states of protein complexes. *J Sep Sci* 34:1692–1695. <https://doi.org/10.1002/jssc.201000869>
38. Puspitasari A, Koganezawa N, Ishizuka Y, Kojima N, Tanaka N, Nakano T, Shirao T (2016) X irradiation induces acute cognitive decline via transient synaptic dysfunction. *Radiat Res* 185:423–430. <https://doi.org/10.1667/RR14236.1>
39. Ishizuka Y, Bramham CR (2020) A simple DMSO-based method for cryopreservation of primary hippocampal and cortical neurons. *J Neurosci Methods* 333:108578. <https://doi.org/10.1016/j.jneumeth.2019.108578>
40. Waltereit R, Dammermann B, Wulff P, Scafidi J, Staubli U, Kauselmann G, Bundman M, Kuhl D (2001) Arg3.1/Arc mRNA induction by Ca²⁺ and cAMP requires protein kinase a and mitogen-activated protein kinase/extracellular regulated kinase activation. *J Neurosci* 21:5484–5493
41. Bindels DS, Haarbosch L, van Weeren L, Postma M, Wiese KE, Mastop M, Aumonier S, Gotthard G, Royant A, Hink MA, Gadella TW Jr (2017) mScarlet: a bright monomeric red fluorescent protein for cellular imaging. *Nat Methods* 14:53–56. <https://doi.org/10.1038/nmeth.4074>
42. McCulloch TW, MacLean DM, Kammermeier PJ (2020) Comparing the performance of mScarlet-I, mRuby3, and mCherry as FRET acceptors for mNeonGreen. *PLoS ONE* 15:e0219886. <https://doi.org/10.1371/journal.pone.0219886>
43. Gurskaya NG, Fradkov AF, Pounkova NI, Staroverov DB, Bulina ME, Yanushevich YG, Labas YA, Lukyanov S, Lukyanov KA (2003) A colourless green fluorescent protein homologue from the non-fluorescent hydromedusa *Aequorea coerulescens* and its fluorescent mutants. *Biochem J* 373:403–408. <https://doi.org/10.1042/BJ20021966>
44. Chen Y, Muller JD, Ruan Q, Gratton E (2002) Molecular brightness characterization of EGFP in vivo by fluorescence fluctuation spectroscopy. *Biophys J* 82:133–144. [https://doi.org/10.1016/S0006-3495\(02\)75380-0](https://doi.org/10.1016/S0006-3495(02)75380-0)
45. Jain RK, Joyce PB, Molinete M, Halban PA, Gorr SU (2001) Oligomerization of green fluorescent protein in the secretory pathway of endocrine cells. *Biochem J* 360:645–649. <https://doi.org/10.1042/0264-6021:3600645>

Publisher's Note Springer Nature remains neutral with regard to jurisdictional claims in published maps and institutional affiliations.